

Inelastic Seismic Demand Mapping of the Regions Using Energy Balance Formulation

A.A. Dindar

Istanbul Kültür University, Department of Civil Engineering, Turkey

C. Yalçın

Boğaziçi University, Department of Civil Engineering, Turkey

E. Yüksel

Istanbul Technical University, Department of Civil Engineering, Turkey

H. Özkaynak

Beykent University, Department of Civil Engineering, Turkey

O. Büyükoztürk

Massachusetts Institute of Technology, Dept. of Civil and Environmental Engineering, USA



SUMMARY:

Seismic hazard maps showing Peak Ground Acceleration (PGA) or Peak Ground Velocities (PGV) or ground motion intensities for a given region are useful information sources to predict possible effects of the future earthquakes on the structures. The current design codes use the PGA and soil condition factors in their procedures. However, strong ground motions create energy which is imparted into the structure. Part of the imparted energy is resisted by the elastic response of the structure while the majority energy must be dissipated by damping and the plastic deformation mechanisms of the structure. Hence, defining the seismic demand of the strong ground motions in terms of the energy parameters can also be considered a new concept in earthquake resistant design philosophy. This study introduces a procedure using Energy Balance Formulation in order to determine the Inelastic Seismic Demand Mapping of a particular region. The procedure is based on the energy spectrum analysis of a Single Degree of Freedom (SDOF) system with Elasto-Perfectly-Plastic (EPP) hysteresis hinging model under the artificially-produced earthquake records that yield the elastic response spectra for that specific region. The obtained energy spectra include different soil conditions, seismic intensities and ductility levels, and are plotted in terms of contour map representations in order to demonstrate the Seismic Energy Demand of the region.

Keywords: Seismic Energy, Hazard Mapping, Inelastic Spectra, SDOF, Constant Ductility

1. INTRODUCTION

Practicing engineers use national and/or regional building codes in the analysis and seismic design of the existing or new structures. Up to now, the strength, displacement or performance-based approaches have been explicitly included in these building codes. Particularly, the analysis of the structures under the seismic excitations is generally based on a response of elastic Single Degree of Freedom System (SDOF) investigated for various strong ground motion records. Even though the response spectrum analysis inherently has several shortcomings (Gupta 1990), the estimation of the seismic hazard for a region described by the soil condition and seismicity have been relied on the use of response spectrum values. Therefore, the analysis of the existing and design of the new buildings in the modern building codes widely use the elastic strength-based seismic demand values in their procedures. However, cumulatively increasing damage of the structural member and its true hysteretic behavior has not yet been explicitly addressed in the current building codes and guidelines.

An energy based approach of characterizing material and structural behavior has the potential to overcome the certain shortcomings in the analysis and seismic design of the structures based on conventional method. The energy induced by the strong ground motion is directly imparted into the structure with certain duration. Throughout this duration, the varying input energy is distributed within the structure in the form of different energy components as shown in Fig. 1.1.

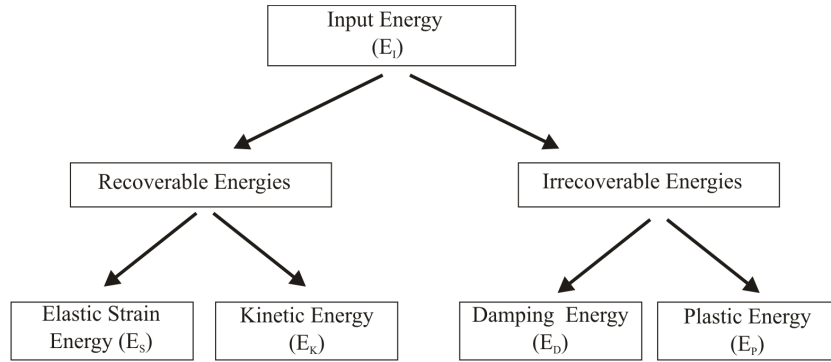


Figure 1.1. Distribution of the imparted seismic energy in the structural system

The structural energy terms resisting the seismic energy couple with both the strength and the deformation characteristics of the structure; hence, they provide a fundamental mechanism in the estimation of the seismic demand due to the ground motions. As seen in Figure 1.1, the seismic Input Energy (E_I) is resisted by two different mechanisms; recoverable and irrecoverable energies. The first mechanism is stored during the seismic action and diminishes at the end. However, the latter is not stored by the structure in any form. It is the irrecoverable energy that is dissipated by the viscous friction of the system and also by the plastic deformation of the structural members. Plastic Energy (E_P) dissipated by the members is directly related to the damage occurrences at the members. Input (E_I) and Plastic (E_P) Energies are invaluable indexes in the computation of the seismic demand since both of them increase cumulatively throughout the duration as seen in Fig.1.2. The total frequency content of the excitation force and also the hysteretic behavior of the member are solely included in the computation.

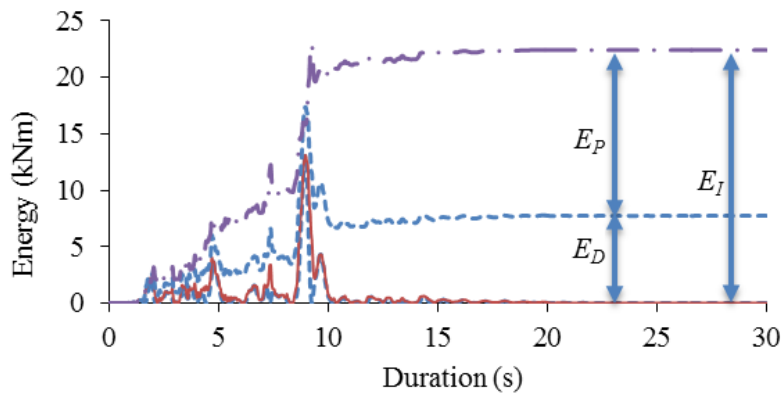


Figure 1.2. Energy time history for inelastic dynamic analysis case

The aim of this study is to determine the Input (E_I) and also Plastic (E_P) Energy-based hazard mapping for a given region, recently studied by Yalçın et al (2008). The hazard maps that were studied in the literature were based on peak ground acceleration (PGA) and velocity values of the soil and also spectral responses of Single Degree of Freedom (SDOF) systems (S_a , S_v , etc). However, it is possible to create a seismic hazard map showing the Input (E_I) energy imparted into the structure and also the Plastic Energy (E_P) dissipated by the structure. This paper discusses a step-by-step procedure for the development of such energy-based hazard maps.

The proposed methodology is limited to cases with certain seismic and soil properties of the region and the characteristics of the structure. In this paper, as an example, the energy-based hazard maps are determined for Istanbul in the Marmara region of Turkey using a SDOF system having Elasto-Perfectly-Plastic (EPP) constitutive behavior model with 5% constant viscous damping.

2. SITE SPECIFIC INFORMATION

Istanbul has a unique geographical situation in terms of crustal plates (Fig. 2.1) which has suffered from several destructive earthquakes in the past due to the North Anatolian Fault (NAF) that is one of the most active strike slip type faults on earth (Şengör et al 2005).

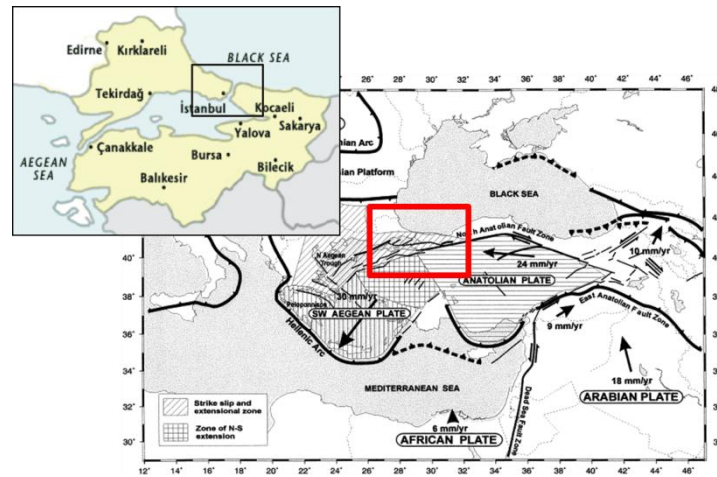


Figure 2.1. Area studied in this study

2.1. Soil Conditions

An extensive micro zonation study has been conducted in Istanbul and its vicinity since 1999 (IMM 2005). Based on the study, the soil conditions with respect to the shear velocity values at 30m depth are depicted in Fig. 2.2.

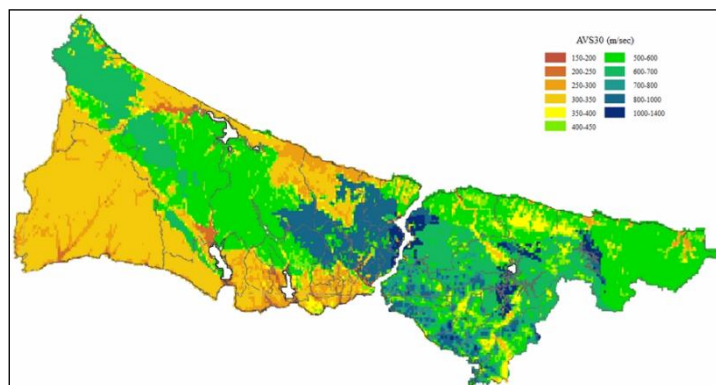


Figure 2.2. Shear velocity map for the city of Istanbul

Based on the soil classification given in Turkish Earthquake Code (2007) with respect to the shear wave velocity, the average shear velocities depicted in Fig.2.2 are classified as in Table 2.1.

Table 2.1. Soil Classifications according to TEC (2007)

| Soil Classification | Soil Condition | Average Shear Velocity at 30m depth (m/sec) |
|---------------------|-------------------------------|---|
| A | Very dense sand, hard clays | 1400-700 |
| B | Dense sands, very stiff clays | 700-400 |
| C | Mid-dense sands, stiff clays | 400-250 |
| D | Loose sands, soft clays | 250-150 |

2.2. Seismic Risk

Earthquake zoning of the cities are defined by Disaster and Emergency Management Agency in Turkey (DEMA). Accordingly, the seismic risk in the city of Istanbul is depicted in Fig. 2.3. As seen in the map, among the heavily populated areas where around 15 million inhabitants live, southern shores of Anatolian and Asian sides are especially vulnerable to potential earthquakes.

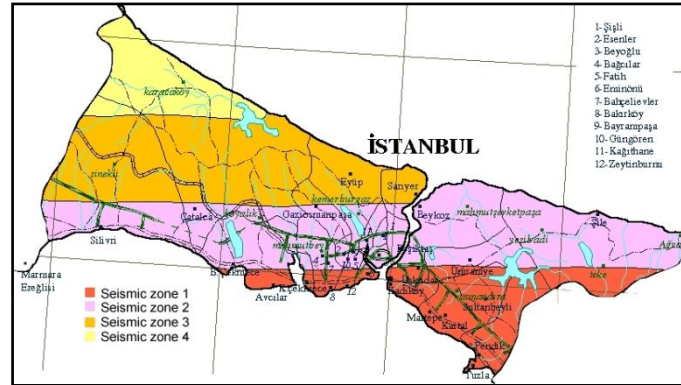


Figure 2.3. Seismic zoning map of Istanbul

Turkish Earthquake Code (TEC2007) considers the earthquake zones those classified by DEMA as the seismic hazard measurement and uses Effective Ground Acceleration (EGA) as the seismic intensity coefficient in the seismic demand analysis. In this study, the seismic intensity is considered in terms of Peak Ground Acceleration (PGA) and the earthquake records used in the determination of the energy spectra analysis are scaled according to the different PGA levels related to the earthquake zones.

3. ANALYSIS BACKGROUND

The seismic hazard assessment mapping proposed in this study is based on the energy terms computed for a SDOF system having different structural attributes (ductility, natural period), soil conditions and seismic intensity.

3.1. Earthquake Records

The proposed seismic hazard mapping is applicable to the sites where some specific information such as soil conditions and seismic intensity is available. The earthquake records to be used in the Energy Time-History (ETH) analysis for spectral values are also needed. Using existing earthquake records suitable to the site is an option. In addition, the artificial earthquake records which are consistent with the site specific response spectrum are another option in the determination of the earthquake excitation.

In this study, artificial earthquake records for four different soil conditions and four different earthquake zones with three alternatives, 48 records, are created. The program used for the artificial records (Sağiroğlu 2004) implements a stochastic simulation process (Shinozuka et al 1999) that complies with the given elastic response acceleration spectrum. In this study, the elastic response spectrum with 5% damping and the 10% probability of exceedance of the design earthquake within a period of 50 years given in TEC (2007) are used. The consistency of a small set of the artificial records is demonstrated in Fig. 3.1.

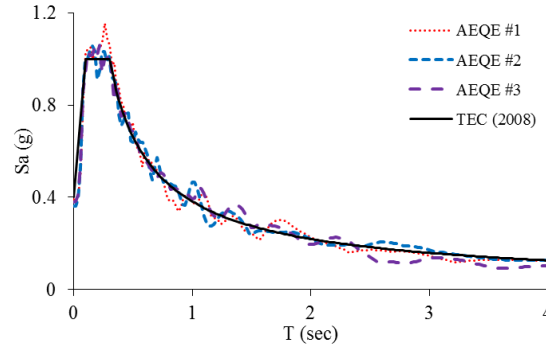


Figure 3.1. Elastic response spectra of TEC (2007) and artificial earthquake records with three alternatives

The 48 artificial earthquake records are taken into the account in computing the Energy-Based seismic hazard mapping as explained below.

3.2. Energy Balance Equation

Energy Balance Equation (EBE) is the concept relied on the conservation of the energy terms throughout the excitation duration. The energy terms given in Fig. 1.1 are computed from the integration of the Equation of Motion (EOM) for a SDOF system with respect to the relative displacement of the mass (Bertero and Uang 1990).

$$\int m\ddot{u}(t)du + \int c\dot{u}(t)du + \int f_s du = -\int m\ddot{u}_g(t)du \quad (3.1)$$

where m is the mass of the structure, \ddot{u} is the relative acceleration, c is the damping coefficient, u is the displacement response, \dot{u} is the relative velocity, f_s is the resisting force and \ddot{u}_g is the ground acceleration.

The terms given in Eqn.3.1 are named as Kinetic (E_K), Damping (E_D), Absorbed (E_A) and Input (E_I) Energies, respectively. Therefore

$$E_K + E_D + E_A = E_I \quad (3.2)$$

The Absorbed Energy (E_A) in Eqn. 3.1 comprises the Strain (E_S) and Plastic (E_P) energies. Plastic (E_P) Energy is computed by subtracting the Strain Energy (E_S) from the Absorbed Energy (E_A), thus,

$$E_P = E_I - (E_K + E_D + E_S) \quad (3.3)$$

Where, Elastic Strain Energy (E_S) is calculated by using the elastic stiffness (k) of the system as follows:

$$E_S = \frac{u^2(t)}{2k} \quad (3.4)$$

This way, Input (E_I) and Plastic (E_P) Energies are directly derived from the Time-History Analysis (THA).

3.3. Energy Time-History Analysis and Spectra

Considering the formulations of each aforementioned energy terms, the Energy Time-History (ETH) analysis of the SDOF system was conducted using the MATLAB programming tool that incorporates

IDARC2D (Reinhorn et al. 1994, version 6.1) as the Time-History (TH) solver engine while considering the constitutive model of the system and ductility levels in the overall computation process. Detailed description of the developed algorithm can be found in Dindar et al (2012).

The displacement ductility (μ) levels defined in the developed computation algorithm are utilized as an iterative TH procedure named as constant ductility approach (Kunnath and Hu 2004). This approach requires a modification of the yield level of the system iteratively until the targeted displacement ductility level converges to the tolerance limits (in this study 1% of the ductility level). Hence, the displacement ductility level is kept constant for each ETH analysis. The displacement ductility (μ) levels were taken as 1 and 2, 4, 6 for elastic and inelastic cases, respectively.

The ETH is repeated on the SDOF system having 5% viscous damping (ξ) and natural periods (T) ranging from 0.05 to 4.0 seconds. At each natural period level, the spectral values Input (E_I) and Plastic (E_P) Energies are obtained from the ETH series covering the entire duration and frequency content of the excitation record as shown in Fig. 3.2.

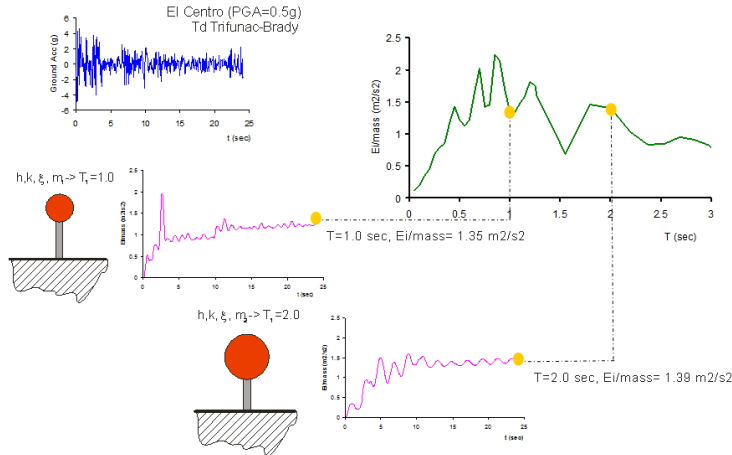


Figure 3.2. Spectral values of the Energy Time History Analysis

For each soil class (Soil A, B, C, and D), constant ductility levels ($\mu=1, 2, 4$ and 6) and seismic intensity levels (Zones 1, 2, 3 and 4), the ETH analysis were conducted for 48 artificial earthquake records. Since there were four different soil class and four seismic intensity levels, the three alternative earthquake records produced slightly changing Input (E_I) and Plastic (E_P) Energy spectra. Therefore, the nominal Input and Plastic Energy spectra values were calculated as the mean plus one standard deviation (84 percentile) of the three spectral values. Following this statistical step, the linear and non-linear regression procedures were applied to the nominal spectra values in order to derive a smoothed spectral form as given in Fig. 3.3.

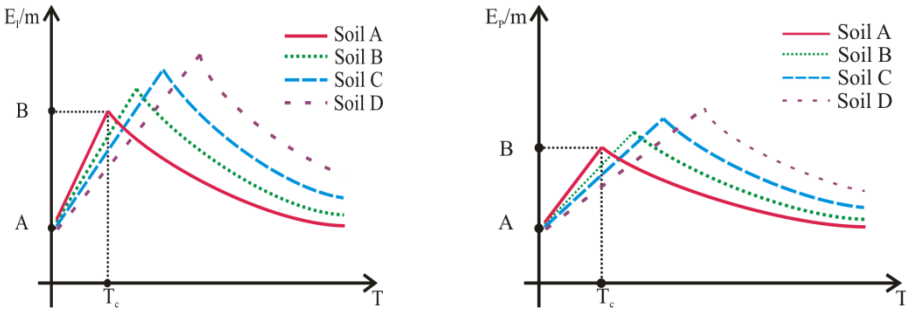


Figure 3.3. Smoothed Input (E_I) and Plastic (E_P) Energy spectra

Similar to the natural earthquake records (Dindar et al, 2012); the artificial earthquake records produced the Input (E_I) and Plastic (E_P) Energy spectra values that can be normalized to the least

seismic intensity case (Seismic Zone 1). The relation between the higher seismic intensity energy spectra values to the least one is the square of the ratio of the PGA values for each earthquake records used in the analysis. Therefore, the Input (E_I) spectra values are formulated as in Eqn.3.5 and Eqn.3.6, respectively.

$$E_I(PGA)/m = (PGA/0.1g)^2 \times E_I(0.1g) \quad (3.5)$$

Where, $E_I(0.1g)$ is

$$E_I(0.1g) = \begin{cases} A + (B - A)(T - 0.05)/(T_C - 0.05) & , T < T_C \\ B(T_C/T)^k & , T \geq T_C \end{cases} \quad (3.6)$$

The Plastic (E_P) Energy spectral values have the similar formulation as in Eqn.3.5 and Eqn. 3.6. The characteristic values for smoothed Input (E_I) and Plastic (E_P) Energy spectra are given in Appendix A.

The Input (E_I) and Plastic (E_P) Energy spectra values calculated for the natural periods ranging from 0.05 to 4.00 second were reckoned as the energy-based spectra library to be used in the construction of the hazard mapping. The spectra library comprises Input (E_I) and Plastic (E_P) Energy spectra values for elastic ($\mu=1$) and inelastic cases ($\mu=2, 4$ and 6).

4. HAZARD MAPPING

Area studied, Fig. 2.2, was divided into 2.5x2.5 km grids where the station points were arranged according to the soil conditions and seismic intensity levels. At each station point, an image process algorithm was developed in MATLAB in order to filter Input (E_I) and Plastic (E_P) Energy spectra values from the energy-based spectra library with respect to the existing soil conditions and seismic intensity. The image process algorithm correlates the two images showing the soil conditions and the seismic zoning and, upon this step, assigns an energy spectra index the station points for the suitable energy spectra. The energy spectra index is the main parameter for filtering the appropriate spectral values from the energy-based spectra library as shown in Fig. 4.1.

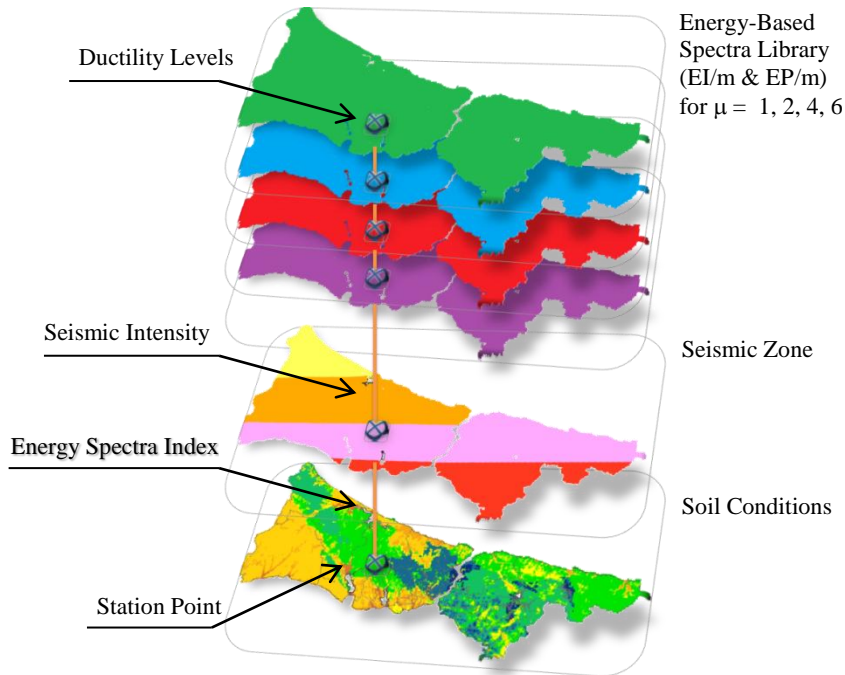


Figure 4.1. Image process to filtering the Input (E_I) and Plastic (E_P) Energy values at the station points

The artificial earthquake records were created according to the spectra given in TEC (2007) that considers the probability of exceedance of the design earthquake within a period of 50 years as 10%. Under these conditions, the seismic hazard maps for T= 0.2 and 1.0 seconds representing the short and 1-second periods are given as the numerical examples for elastic ($\mu=1$) and inelastic cases ($\mu=2, 4$ and 6) in Figs. 4.2-4.5.

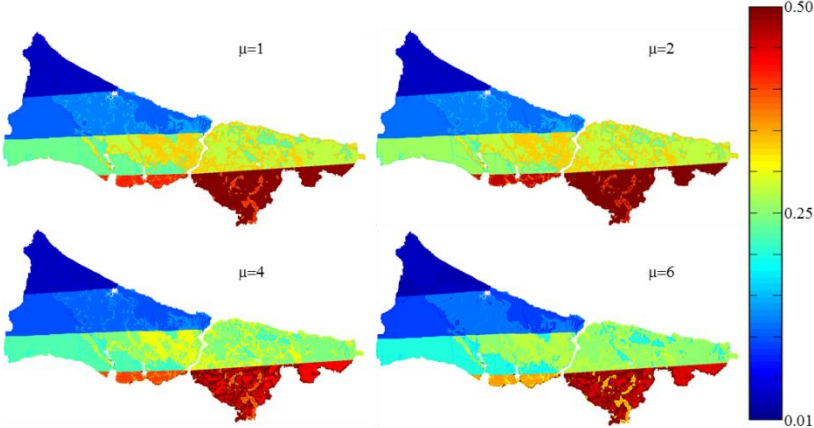


Figure 4.2. Mass normalized Input Energy (E_I) seismic hazard map for T=0.2

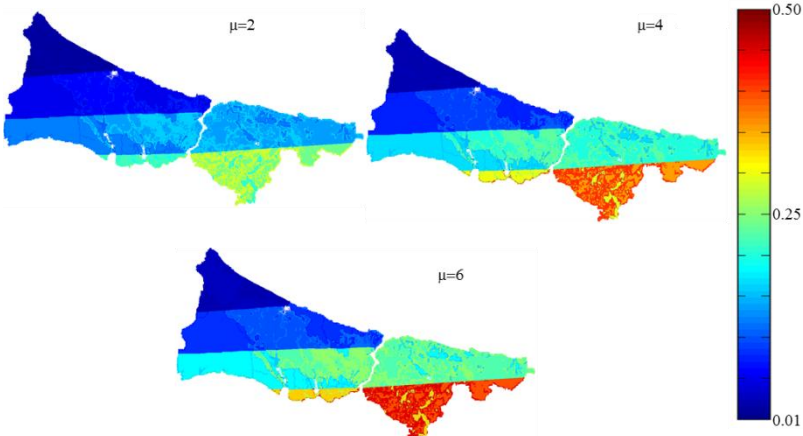


Figure 4.3. Mass normalized Plastic Energy (E_P) seismic hazard map for T=0.2

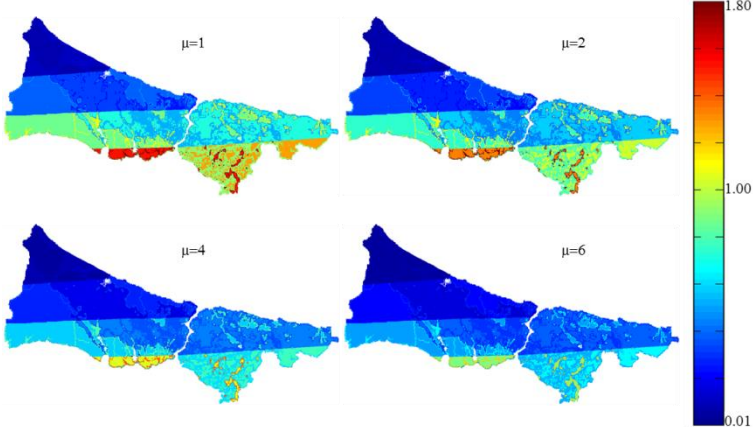


Figure 4.4. Mass normalized Input Energy (E_I) seismic hazard map for T=1.0

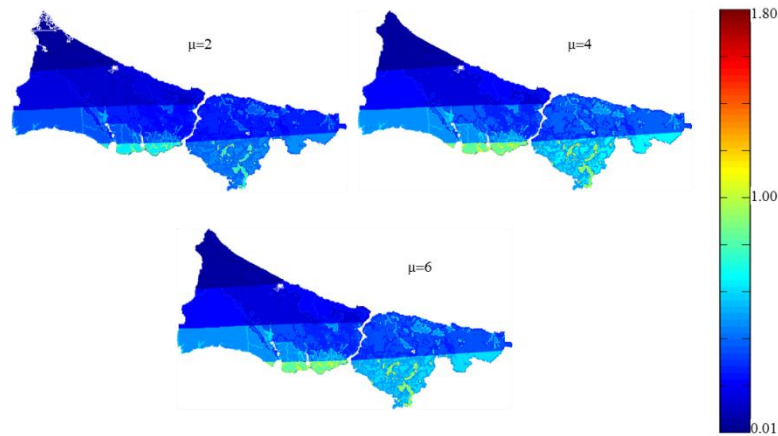


Figure 4.5. Mass normalized Plastic Energy (E_p) seismic hazard map for $T=1.0$

5. CONCLUSION

In this study, a novel procedure of plotting the seismic hazard mapping based on Input (E_I) and Plastic (E_P) Seismic Energy demand is introduced. The energy terms used in the study are derived from the Energy-Balance formulation. The smoothed Input (E_I) and Plastic (E_P) Energy spectra are directly computed for a SDOF system under the excitation of a large set of artificial earthquake records created according to the elastic response spectrum defined in TEC (2007). An extensive spectral energy demand library comprises the parameters of natural period ranging between $T=0.05$ to 4.00 sec, four different soil conditions, seismic intensity ($PGA=0.1$ g) and displacement ductilities ($\mu= 1, 2, 4, 6$) are developed based on the conducted Energy Time History (ETH) analysis. For the higher seismic intensity levels, the spectral values are normalized to the least intensity level ($PGA=0.1g$). To obtain the spectral values at higher seismic intensities, the spectral energy demand values are calculated by quadratic formulation.

The procedure described in the study is indeed applicable to any site where the soil conditions and seismic intensity level information are available. In this study, city of Istanbul and its vicinity is chosen as a case study where the seismic risks are very high. The soil conditions and seismic risk maps are processed together in order to assign the energy spectra index for each station points. According to the energy spectra index, the station points located at 2.5×2.5 km grid intersections in the area studied are related to the appropriate Input (E_I) and Plastic (E_P) Energy values from the energy demand spectra library. Once the station point's location and the Energy Demand spectra is associated to the Energy spectra index, it is just a matter of plotting the seismic hazard map with the spectral values calculated for the targeted displacement ductility level (elastic or inelastic) and the natural period of the structures within the study area. Thus, a new method is introduced to the practicing engineer to estimate the total Input (E_I) and Plastic (E_P) Energy values that are calculated by multiplying the spectral values by the mass of the existing and new structures located to be analyzed or designed in the seismic areas.

ACKNOWLEDGEMENT

This study is financially supported by Istanbul Kültür University Scientific Research Committee. This support is hereby gratefully acknowledged.

REFERENCES

Bertero, V.V. and Uang, C.M. (1990). Evaluation of Seismic Energy in Structures. *Earthquake Engineering and Structural Dynamics* 19, 77-90.

- Dindar, A.A., Yalçın, C., Yüksel, E., Özkaynak, H. and Büyüköztürk, O. (2012). The Use of Earthquake Energy Demand in Seismic Design of Structures, Submitted to Earthquake Spectra on March 16th, 2012.
- Gupta, A.K. (1990), Response Spectrum Method, CRC Press Inc., USA.
- Istanbul Metropolitan Municipality (2005), Fundamental Geology of Istanbul, Technical Report in Turkish, Istanbul, Turkey.
- Kunnath, S.K. and Hu, Q. (2004). Evaluation of Cyclic Demand in Ductile RC Structures, 13th World Conference on Earthquake Engineering, Vancouver, Canada, Paper No.290.
- Sağiroğlu, S. (2004), Statistical analysis of the costs and benefits of various retrofitting schemes for buildings subjected to earthquakes, M.Sc. Thesis Boğaziçi University, Istanbul, Turkey.
- Shinozuka, M., Deodatis G., Zhang R., Papageorgioud A.S. (1999). Modeling, synthetics and engineering applications of strong earthquake wave motion. Soil Dynamics and Earthquake Engineering 18, 209–228.
- Şengör, A.M.C., Tüysüz, O., İmren, C., Sakıncı, M., Eyidoğan, H., Görür, N., Pichon, X.L. and Rangin, C. (2005). The North Anatolian Fault: A New Look. Annual Review of Earth and Planetary Sciences, 33: 37-112
- Reinhorn, A.M., Kunnath, S.K. and Valles, R.E. (1994), IDARC2D: A Program for the Inelastic Damage Analysis of Buildings, National Center for Earthquake Engineering Research, N.Y, USA.
- Turkish Earthquake Code (TEC) (2007), Specification for Structures to be Built in Disaster Areas, Ministry of Public Works and Settlement, Government of the Republic of Turkey, Ankara.
- Yalçın, C., Yüksel, Dindar, A.A., E., Özkaynak, H. and Büyüköztürk, O. (2008). Seismic energy demand mapping of regions using energy-based methodology, 14th World Conference on Earthquake Engineering, Beijing, China, Paper No.07-0014.

APPENDIX

The coefficients of the proposed Input (E_I) and Plastic Energy (E_P) spectra directly derived from the artificial earthquake records compatible with elastic response spectrum given in Turkish Earthquake Code (2007).

| Parameters | Soil A | | Soil B | | Soil C | | Soil D | |
|------------|---------|---------|---------|---------|---------|---------|---------|---------|
| | E_I/m | E_P/m | E_I/m | E_P/m | E_I/m | E_P/m | E_I/m | E_P/m |
| $\mu=1$ | | | | | | | | |
| Tc | 0.50 | 0.00 | 0.45 | 0.45 | 0.40 | 0.40 | 0.35 | 0.35 |
| A | 0.0085 | 0.0000 | 0.0091 | 0.0044 | 0.0078 | 0.0064 | 0.0048 | 0.0043 |
| B | 0.0933 | 0.0000 | 0.0821 | 0.0399 | 0.0668 | 0.0508 | 0.0570 | 0.0524 |
| K | 0.71 | 0.00 | 0.63 | 0.68 | 0.61 | 0.58 | 0.54 | 0.52 |
| $\mu=2$ | | | | | | | | |
| Tc | 0.70 | 0.00 | 0.60 | 0.60 | 0.55 | 0.55 | 0.45 | 0.45 |
| A | 0.0076 | 0.0000 | 0.0077 | 0.0037 | 0.0068 | 0.0056 | 0.0045 | 0.0039 |
| B | 0.1069 | 0.0000 | 0.0923 | 0.0447 | 0.0746 | 0.0617 | 0.0675 | 0.0590 |
| K | 0.84 | 0.00 | 0.73 | 0.80 | 0.71 | 0.66 | 0.60 | 0.55 |
| $\mu=4$ | | | | | | | | |
| Tc | 0.85 | 0.00 | 0.75 | 0.75 | 0.70 | 0.70 | 0.65 | 0.65 |
| A | 0.0066 | 0.0000 | 0.0070 | 0.0033 | 0.0063 | 0.0047 | 0.0040 | 0.0036 |
| B | 0.1119 | 0.0000 | 0.1095 | 0.0515 | 0.0876 | 0.0663 | 0.0760 | 0.0720 |
| K | 0.92 | 0.00 | 0.92 | 0.92 | 0.82 | 0.71 | 0.75 | 0.76 |
| $\mu=6$ | | | | | | | | |
| Tc | 1.10 | 0.00 | 1.00 | 1.00 | 0.90 | 0.90 | 0.85 | 0.85 |
| A | 0.0058 | 0.0000 | 0.0060 | 0.0027 | 0.0055 | 0.0042 | 0.0038 | 0.0034 |
| B | 0.1311 | 0.0000 | 0.1197 | 0.0581 | 0.0989 | 0.0756 | 0.0863 | 0.0782 |
| K | 1.20 | 0.00 | 1.10 | 1.00 | 0.95 | 0.91 | 0.88 | 0.85 |